ADVANCED MATERIALS

Supporting Information

for *Adv. Mater.*, DOI 10.1002/adma.202302069

Renally Clearable Ultraminiature Chain-Like Gold Nanoparticle Clusters for Multimodal Molecular Imaging of Choroidal Neovascularization

Van Phuc Nguyen, Wei Qian, Josh Zhe, Jessica Henry, Mingyang Wang, Bing Liu, Wei Zhang, Xueding Wang and Yannis M. Paulus**

Supplementary Information

Renally Clearable Ultraminiature Chain-Like Gold Nanoparticle Clusters for Multimodal Molecular Imaging of Choroidal Neovascularization

Van Phuc Nguyen[1], Wei Qian[2], Josh Zhe[1], Jessica Henry[1], Mingyang Wang[3], Bing Liu[2], Wei Zhang[3], Xueding Wang[3]*, and Yannis M. Paulus[1,3*]

[1]Department of Ophthalmology and Visual Sciences, University of Michigan, Ann Arbor, MI 48105, USA
[2]IMRA America, Inc., 1044 Woodridge Ave., Ann Arbor, MI 48105, USA
[3]Department of Biomedical Engineering, University of Michigan, Ann Arbor, MI 48105, USA

[*]Corresponding authors.

Yannis M. Paulus, M.D., F.A.C.S.

Department of Ophthalmology and Visual Sciences

Department of Biomedical Engineering

University of Michigan

1000 Wall Street

Ann Arbor, MI 48105, USA

Email Address: ypaulus@med.umich.edu

Xueding Wang, Ph.D.

Department of Biomedical Engineering

Department of Radiology

University of Michigan

Email Address: xdwang@umich.edu

This PDF file includes:

Supporting text
Figs. S1 to S6
Captions for Movie S1 to S3
Supplementary References

Other Supplementary Materials for this manuscript include the following:

Movie S1 to S3

Supporting Information Text

Supplementary Note 1: Chemical materials and Instrumentations: Ketamine and xylazine were obtained from Michigan Medicine pharmacy. Indocyanine green (ICG) and fluorescein sodium were obtained from Akorn (Lake Forest, IL, USA). Rose Bengal solution was sourced from Sigma-Aldrich (Sigma, St. Louis, Mo, USA). Thiol-terminated polyethylene glycol (PEG-SH) powder was ordered from Creative PEGWorks (Chapel Hill, NC, catalog # PLS-605). The PEG 2k-SH was reconstituted by dissolving it in deionized (DI) water. Cysteine-modified $(RGD)_4$ peptides (RGDRGDRGDRGDPGC) and CALNN pentapeptide ligand were custom-synthesized by RS synthesis LLC (Louisville, KY) and had a purity higher than 95%. Cysteamine was received from Sigma-Aldrich and similarly had a purity higher than 95%. These reconstituted solutions were all used within twelve hours of mixing with DI water. The fine gold (99.99% purity) with dimension of 16 mm×8 mm×0.5 mm was obtained from Alfa Aesar (Ward Hill, MA). Propidium iodide (PI), Annexin-V FITC, 3-(4,5-Dimethyl-2-thiazolyl)-2,5-diphenyl-2H-tetrazolium bromide (MTT), tylosin, sodium bicarbonate, dimethyl sulfoxide (DMSO), and Dulbecco's modified eagle's medium (DMEM) were purchased from Sigma-Aldrich (Sigma, St.

Louis, Mo, USA). EndoGRO was obtained from Vec Technologies (Rensselaer, NY, USA). Antibiotics/antimycotics, phosphate-buffered saline (PBS), trypsin–ethylenediaminetetraacetic acid (trypsin-EDTA), and fetal bovine serum (FBS) were obtained from Gibco BRL, Life Technologies (Grand Island, NY, USA). No chemicals purchased for these experiments required further purification.

An UV-3600 spectrophotometer was used to determine the absorption spectra of the synthesized GNC (Shimadzu Corp., Japan). A Fourier transformed infrared spectroscopy (FTIR) spectrometer was implemented to assess the infrared spectra of the samples. TEM was used to record images of colloidal GNPs using an accelerating voltage of 100 kV. DLS analyses of zeta potential and nanoparticle hemodynamic diameter size was performed using Nano-ZS90 Zetasizer (Malvern Instrument, Westborough, MA).

Supplementary Note 2: Fabrication of PEGylated and RGD Peptide-conjugated ultraminiature Gold Nanochains for Molecular imaging

Physical Production of Colloidal Gold Nanoparticles (GNPs): Raw, agent-free spherical colloidal GNPs were first produced via femtosecond laser ablation of gold target in the same manner as described in previous literature(*1, 2*). These would be used for the fabrication of GNC. As shown in Fig. 1a, the size of the produced GNPs could be accurately adjusted by optimizing laser fluence, repetition rate, pulse duration, and wavelength. The ytterbium-doped femtosecond fiber laser system (FCPA μJewel D-1000, IMRA America, Ann Arbor, MI) was used to illuminate the bulk gold sample. The laser system provided a pulsed fluence of 10 μJ with a pulse duration of 700 fs and a repetition rate of 100 kHz. An objective lens was used to focus the

laser beam on the surface of the sample. The focus spot size was about 50 μm. GNPs were moderately oxidized by oxygen present to form Au-O in the solution during pulsed laser ablation. Sylvestre, J.-P. *et al.(3)* have discribed that the oxidized Au were hydroxylated and underwent proton transmission to provide a negative superficial charge ($Au\text{-}O^-$). No stabilizing agents were needed to maintain their colloidal stability, which was crucial for the one-dimensional (1D) GNC self-assembly process. Disperse GNPs (7-8 nm and 20 nm) were generated for use in experiments. The fabricated particles had a narrow particle distribution and reached the peak absorption at 520 nm.

Formation of GNC from GNP monomers: To perform the self-assembly process forming GNC, 20 nm and 7-8 nm in diameter spherical GNP monomers were modified with a pentapeptide, CALNN, and cysteamine. The minimum quantity of CALNN peptide and cysteamine molecules was used in order to form stable chains of GNPs. Minimizing the quantity of these compounds allows for additional surface area to be available for further modification with PEG molecules, ICG dyes, and RGD peptides. This was executed in a sequential manner by first adding CALNN and then cysteamine. Bonds were formed between the bare GNP monomers and these two compounds due to the strong anchoring of Au-S bonds, which formed the connection between Au and cysteamine and CALNN. These two ligands, CALNN and cysteamine, aided in the self-assembly process, and CALNN additionally improved nanoparticle colloidal stability by enhancing interparticle electrostatic repulsion(*4*). This stability is important for achieving optimal repulsive potential and attractive potential between GNP monomers to form the chain-like gold nanoparticle clusters(*4, 5*).

The experiment involved mixing either the 20 nm or 7-8 nm colloidal GNP monomers with CALNN peptides and then keeping them undisturbed at 20 ^{o}C. After 2 h, GNPs were sufficiently conjugated to CALNN ligands, and cysteamine molecules were then added. This mixture was retained undisturbed until the color of the suspension solution transformed from red-pink to blue. This color change usually occurred at 1 day or few days post combination of cysteamine, which served as sign of successful self-assembly of GNP monomers into GNC. The solution was then centrifuged to produce a pellet. The supernatant was removed, and the final OD was adjusted to 10 through the addition of DI water.

PEGylation and RGD conjugation of GNC: The raw GNC composed of either 20 nm or 7-8 nm diameter GNP monomers were functionalized with PEG and RGD to for targeting CNV in rabbit eyes. RGD peptides coated on the surface of GNC provide molecular imaging by binding with complementary proteins including α_5 and α_v integrins. To functionalize the GNC, 20 µL PEG-2k-SH was first added to 5 mL of the mixture of raw clusters (OD 10 at 605 nm) at 1 mM. The sample was unmoved at room temperature for 2 h to allow conjugation via Au-S bonds. Next, 60 µL RGD peptides were added to the mixture at a concentration of 1 mM. This solution was permitted to incubate for 2 h at 21 ^{o}C to allow junction of RGD to vacant areas on GNC. To conclude, the final solution was moved to a 15 mL centrifuge tube and centrifuged at 1000 g for 0.5 h. The resulting pellet formed was resuspended in 4 mM borate buffer (pH 8.2) in 5 mg/mL BSA. The final OD of the colloidal solution of PEGylated and RGD ligand-conjugated GNC was approximately 100.

Supplementary Note 3: Characterization of GNC-RGD: To characterize the colloidal GNC-RGD, UV-Vis absorption spectroscopy, TEM, FTIR, and DLS were used. All measurements were obtained at room temperature. UV-Vis absorption spectrum of GNC-RGD was characterized between 350 and 800 nm. TEM analysis was performed at an accelerating voltage of 100 kV to provide visualization of the colloidal GNC cluster-RGD. To measure the hydrodynamic diameter, DLS measurements were taken. FTIR was used to produce the infrared spectra of bare GNC, PEG, and GNC-RGD. The results from this assay verified PEG was successful conjugated to the surface of GNC-RGD.

Supplementary Note 4: Cytotoxicity assessments

Cell culture preparation: Dr. David Antonetti generously donated a human retinal pigment epithelial cell line with differentiated properties (ARPE-19) cells. Human umbilical Vein Endothelial Cells (HUVEC) were obtained from Dr. Abigail Fahim. HeLa cells were purchased from ATCC (ATCC, Manassas, Virginia, USA). DMEM including 10% FBS and antibiotics was used to culture HeLa cells. The ARPE-19 cells were treated with DMEM-F12 mixed with 10% FBS, EGF (20 ng/mL), antibiotics/ antimycotics (10 mL), sodium bicarbonate (1.18 g), EndoGRO (200 mg), heparin (90 mg), and tylosin (1 mL). The vascular cell basal medium (VCBM) was used for HUVEC cells and obtained from ATCC (Manassas, Virginia, USA). The media was added with endothelial cell growth kit including bovine brain extract (BBE): 0.2%, rh EGF: 5 ng/mL, L-glutamine: 10 mM, heparin sulfate: 0.75 Units/mL, hydrocortisone: 1 µg/mL, ascorbic acid: 50 µg/mL, fetal bovine serum: 2%. To see the elevation growth of HUVEC cells, the cells were cultured with VCBM combined with Endothelial Cell Growth Kit-VEGF (rh

VEGF: 5 ng/mL. rh EGF: 5 ng/mL, rh FGF basic: 5 ng/mL, rh IGF-1: 15 ng/mL, L-glutamine: 10 mM, heparin sulfate: 0.75 Units/mL, hydrocortisone: 1 µg/mL, ascorbic acid: 50 µg/mL, fetal bovine serum: 2%). The plate was maintained at 37 °C and a humidified atmosphere of 95% air and 5% CO_2. The culture medium in the cell plated were changed 2 times per week. ARPE-19, and HeLa cells were collected using 0.25% trypsin-EDTA after the plates had reached 70-90% confluence and centrifuged for 5 min at 500 rpm.

Cellular uptake: Cellular uptake analysis of RGD-conjugated ultraminiature GNC was performed on ARPE-19, HUVEC and HeLa cells. 2×10^5 cells were cultured on 35 mm microplates and incubated for 24 h. Then, the culture medium was changed with one containing GNC at 100 µg/mL. After 24 h of incubation, unbound nanoparticles were washed with PBS prior to staining with lysotracker, phalloidin and DAPI. 1 µM of lysotracker Red was added to the cell media and incubated for 20 min at 37 ^oC and 5% CO_2. The sample was washed 2 times with cold PBS and then fixed with 2% formaldehyde and maintained at 37 °C for 20 mins. Afterwards, the cells were stained with 2.5 µL of phalloidin in 100 µL of mixture BSA, glycine and formalin for 25 min. The samples were subsequently rinsed two times with cold PBS before adding 500 µL of 10 µg/mL DAPI solution. The plates were further incubated in a 37 °C, dark environment for 20 minutes. The stained cells were washed with cold PBS three times prior to analysis with the Leica Stellaris 8 (Leica, Wetzlar, Germany).

***In vitro* biocompatibility and cell viability of ultraminiature and large GNC-RGD:** GNC-RGD were tested in HeLa, HUVEC, and ARPE-19 cells to verify cytotoxicity and

biocompatibility. The assays were performed by culturing 2×10^4 cells/well in 96-well microplates. The samples were kept in incubator until 80% confluence was achieved. The plates were rinsed with PBS solution and then the ultraminiature or large GNC-RGD at several concentrations ranging from 0 (control) to 500 µg/mL was added to the cell's medium. To evaluate the influence of incubation time on cells survival, the cells were kept for 24 h and 48 h at 37 °C in humidified atmosphere of 5% CO_2 and 95% air.

MTT assay: Typical methyl tetrazolium (MTT) analysis was performed to assess the potential toxicity of PEG-GNPs. The samples were incubated for different times at a range of concentrations with either ultraminiature or large GNC-RGD. The cells were then washed with cold PBS and then replaced with MTT reagent (100 µL,1 mg/mL), and kept in dim light location for 4 h. The plates were move to 37 °C where mitochondrial succinate dehydrogenase in live cells caused the transition of MTT into purple. The crystals were dissolved by DMSO and then kept at 21 ^{o}C for 20 min. Once the color distribution had homogenized, the optical density (OD) was excited at 570 nm by a microplate reader (Epoch, Biotek USA). Cell viability based on this assay was computed and compared to the non-treated, control group using Formula (1).

$$P = \frac{OD\,experimental\,group}{OD\,control\,group} \times 100 \qquad \textbf{(1)}$$

Flow cytometric analysis: Flow cytometry was used to determine the degree of apoptosis and necrosis in GNC cluster-RGD treated cells with and without laser illumination. The assay visualized any change in granularity or size of cells, indicating potential cell damage including apoptosis or necrosis. Apoptosis is present when nuclear fragmentation, DNA loss, or cell

shrinkage is apparent. The cells are classified as necrotic or apoptotic by the light scattering effect of the cells. The Annexin-V FITC Apoptosis Detection Kit was added to samples of cells incubated with either ultraminiature or large GNC-RGD. Cells were trypsinized and harvested with a centrifuge (1500 rpm for 3 min) after being incubated for 24 or 48 h with either ultraminiature or large GNC-RGD. 1X binding buffer was added to re-suspend the cells (500 µL). Then, PI solution (10 µg/ml) and Annexin-V FITC were added. The sample was incubated for 15 minutes. The sample was mixed with 1 mL of PBS and analysis with flow cytometry. Samples of untreated cells no staining, untreated cells with PI, and untreated cells with Annexin-V FITC were also prepared for a control group. The flow cytometry assay was performed, and the analysis yielded quantitative information on cellular status.

Stability of ultraminiature GNC-RGD

Photostability analysis of ultraminiature and large GNC-RGD: A group of 8 samples were prepared to investigate the photostability of GNC-RGD after laser irradiation. The samples included 100 µL of either ultraminiature or large GNC-RGD at 5 mg/mL. The samples were illuminated with one of four possible nanosecond laser fluences at 650 nm: 0.005, 0.01, 0.02, and 0.04 mJ/cm^2. The resulting samples were analyzed by measuring their UV-Vis absorption spectra.

Circulation kinetics and bioavailability of ultraminiature and large GNC-RGD: The circulation times of ultraminiature and large GNC-RGD were compared by gathering blood

samples from rabbits *in vivo*. This assay was performed by intravenously (IV) injecting rabbits in the marginal ear vein with 400 µL of either ultraminiature or large GNC-RGD at 5 mg/mL. Samples were gathered pre and 15, 45, 60 min and 2, 4, 8, 16, 24, 48, 72 h, and days 4, 5 and 7 after administration of GNC-RGD. For analysis, the samples were melted in hydrochloric and nitric acid prior to using an inductively coupled plasma mass spectrometer (iCAP™ RQ ICP-MS, Thermo Fisher Scientific, Bremen, Germany).

***In Vivo* Toxicity of GNC-RGD:** Toxicity of ultraminiature and large GNC cluster-RGD was assessed in laboratory mice. Eighteen groups of animals were prepared with N=3 per group including a control group. The experimental arms included bare colloidal GNP monomers and GNC-RGD composed of either 20 nm or 5 nm diameter GNP monomers at 2.5, 5, 10, 20, 2200, and 8800 mg/kg. 500 µL of each size and structure of gold nanoparticles were prepared for injection into the tail vein. The mice were weighed pre and post injection for 1 week. The mice were then euthanized, and blood (in 600 µl blood collection tubes), heart, lung, kidney, liver, and spleen samples were gathered, washed with PBS, weighed, and placed in -40 ^{o}C for storage. The samples were then analyzed for gold quantity using ICP-MS. Samples were all centrifuged for 10 min at 1300 rpm and then stored at 4 ^{o}C for chemistry panel analysis.

ICP-MS Biodistribution Analysis: The procedure resembled the west digest protocol for processing and digesting tissue samples for ICP-MS quantification. In summary, 0.2 g of an organ sample or 2 mL of a fluid sample was dissolved in 1 mL of nitric acid (67%) at 100 ^{o}C for 3 min. Hydrochloric acid (3 mL) was poured into the sample and then heated at 180-200 ^{o}C until

the sample had dried to 1 mL. The sample were mixed with 4 mL DI water and filtered using a 0.22 µL filter (Merc Millipore Ltd., Co. Cork, Ireland). The solutions were diluted with an additional 5 mL DI water and then analyzed using an ICP-MS device ((iCAP™ RQ ICP-MS, Thermo Fisher Scientific, Bremen, Germany).

Histological analysis: Rabbits were euthanized fourteen days post IV injection of either ultraminiature or large GNC by an intravenous injection of pentobarbital. The resulting tissue samples were used to measure the toxicity of GNC-RGD *in vivo*. The eyes, heart, liver, spleen, and kidneys were all extracted aseptically for histological analysis in both the treated and control groups. The samples were prefixed with 10% neutral buffered formalin (VWR, Radnor, PA) for 24 h. Davidson's fixative solution (Electron Microscope Sciences, PA, USA) was added to the eye samples to prevent retinal detachment, and this was allowed to rest for 8 h. Afterwards, the eye was fixed with 50% of alcohol for 8 h and 70% of alcohol overnight. The samples were then embedded in paraffin. These were then further cut into 4 µm thick samples and stained with terminal deoxynucleotidyl transferase dUTP nick end labeling (TUNEL) assay and hematoxylin and eosin (H&E) under standard conditions by a Leica autostainer XL (Leica Biosystems, Nussloch, Germany). Leica DM6000 light microscope (Leica Biosystems, Nussloch, Germany) was used to examine the slides for evidence of apoptotic or necrotic cells.

Transmission Electron Microscopy: Liver tissues were collected and divided using a razorblade into $0.5\times0.5\times2$ mm^3 sections for electron microscopy assessment. The samples were next added to 0.1 M Sorensen's phosphate buffer (pH = 7.4) and 2.5% glutaraldehyde to be fixed

in a 4 ^{o}C environment for 24 h. The samples were then washed three times with 0.1 M Soren's buffer for 15 minutes each. The samples were then added to 1% osmium tetroxide in 0.1 M Sorensen's buffer for post-fixation at room temperature for 1 h. The previous step was then repeated (rinse three times with 0.1 M Sorensen's phosphate buffer for 15 min). To dehydrate the samples, 25, 50, 70, 95 and 100% of acetone was added to the samples for 5 min. The samples were sliced using ultra-microtome into ultrathin, 70 nm sections after they were polymerized for 24 h at 60 ^{o}C. Sections were then mounted without base layers onto 200 mesh fine bar hex grids. The sections were then stained for 10 min at 56 ^{o}C with lead citrate and uranyl acetate. The transmission electron microscope (TEM) images were captured using a JOEL-JEM 1400 Plus device (Japan Electron Optic, Tokyo, Japan).

Supplementary Note 5: Sample Preparations

Phantom preparation: Phantom samples (N=3) were prepared in silicone tubes (inner diameter = 0.30 mm and outder diameter = 0.64 mm) to examine PAM signal *in vitro* of GNC-RGD. The tubes were filled with different concentrations of either ultraminiature or large GNC-RGD solution including 0 (saline control), 0.04, and 0.08 mg/mL. Optical adhesive was used to seal the distal ends of each tube. For PAM imaging, the phantoms were then placed on a coverslip and then into a degasses water tank to inhibit cavitation. To examine OCT signal *in vitro*, capillary glass tubes (inner diameter = 0.30 mm and outder diameter = 0.54 mm) were filled with 0 (saline control), 0.02, 0.04, and 0.08 mg/mL of either ultraminiature or large GNC-RGD suspension solution (N = 3). To analysis the OCT signal as a function of concentrations, glass

tubes were filled with ultraminiature and large GNC at different concentration ranging from 1–5×10^8 pg/mL. Both ends of the glass tubes were capped with optical adhesive.

Supplementary Note 6: Animal model Preparation:

Animal model characteristics: All animal studies were in accordance with the Association for Research in Vision and Ophthalmology (ARVO) Statement on the care and use of laboratory animals in Ophthalmic and Vision Research. The rabbit experimental protocol was first approved by the Institutional Animal Care and Use Committee (IACUC) of the University of Michigan (Protocol number: PRO00010388, PI: Y. Paulus). 2- to 3-month-old white New Zealand rabbits weighing 2.7 to 3.2 kg were bred and generously donated by the Center for Advanced Models and Translational Sciences and Therapeutics (CAMTraST) at the University of Michigan.

Laser-induced retinal vein occlusion (RVO) model: The laser-induced retinal vein occlusion (RVO) in rabbit was generated in accordance with the protocol by Nguyen *et al.* and Oncel *et al*.(*6*). To prepare the model, a contact lens (Volk Optical Inc, Mentor, OH, USA) coated with Gonak gel (Akorn, Lake Forest, IL, USA) was placed directly on the cornea. The target retinal vessels were identified. Rose Bengal solution was gradually administrated into the rabbits. 5 second post injection, the rabbit eye received laser irradiation (Vitra 532nm, Quantel Medical, Cournon d'Auvergne, France). The laser had a wavelength of 532 nm, power of 150-300 mW, aerial diameter of 75 μm, and irradiation time of 0.5 s per spot. The power was initially 150 mW

with the system applying 20 shots to the same location until the blood flow had ceased. The laser at 300 mW power was then used for another 20 shots to prevent any reperfusion.

CNV model induced by subretinal injection of vascular endothelial growth factor (VEGF): This second model of subretinal injection was prepared to serve as a comparison to the RVO model. The rabbit eyes were subretinally injected with 700 ng VEGF-165 (100 µg/mL) (Shenandoah Biotechnology, Warwick, USA) in 20 µL of Matrigel (Corning, NY, USA).

Supplementary Note 7: Animal model imaging

Color fundus photography and fluorescein angiography (FA): Color fundus photography was employed to image the major retinal vasculature pre and post laser treatment or subretinal administration (Topcon 50EX, Topcon Corporation, Tokyo, Japan). The color fundus was useful to orient to the regions of laser irradiation to monitor changes post treatment. To monitor the laser-induced model, the dynamic changes and percentage of blood perfusion information was useful in tracking neovascularization and other changes. For the subretinal injection model, vessel density was a measure of the efficacy of the treatment.

Using the Topcon 50 EX fundus photography system, 0.2 mL fluorescein dye (Akorn, Lake SegForest, IL, USA) was administered intravenously into the rabbit. FA images were particularly captured immediately after laser irradiation to determine if the vessel had occluded as anticipated. Late phase FA images were achieved each minute for 15 minutes to monitor leakage and potential neovascularization.

Multimodal molecular PAM and OCT imaging: The multimodal photoacoustic microscopy (PAM) and OCT system has been reported in detail in our previous studies(*7-8*). In brief, a turnable nanosecond pulsed laser with a pulse duration of 3 – 6 ns and repetition rate of 1 kHz was used to illuminate the samples (NT-242, Ekspla, Lithuania). The optical wavelength can be adjusted from 405 – 2600 nm. The laser light was focused, filtered, and collimated by a beam collimated composed of a focusing lens (focal length 250 mm), a collimating lens (focal length 30 mm), and a pinhole (diameter 50 μm). The resulting light had a circular shape (~2 mm). The laser light was then transmitted through a 2D galvanometer and optics system including scan lens (f=36 mm) and ocular lens (f=10 mm) before focus on the rabbit's fundus.

The laser light wavelength at 578 nm had a fluence on the eye of 0.01 mJ/cm^2 at half of the American National Standards Institute (ANSI) limit. A 27.0 MHz ultrasound sensor was utilized to record the PA signals (Optosonic Inc., Arcadia, CA, USA). The PA signals were magnified using an amplifier (AU-1647, L3 Narda-MITEQ, NY). The axial resolution was 37.0 μm and transverse resolution was 4.1 μm. The signal was then digitized using a PX1500-4 digitizer (Signatec inc., Newport Beach, CA). After digitization, the recorded data was processed to rebuild two-dimensional and three-dimensional volumetric PAM images using Amira software.

The optical coherence tomography (OCT) was an altered commercially available OCT system (Ganymede-II-HR, Thorlabs, Newton, NJ) as described previously. The modification involved inserting an ophthalmic lens after the scan lens and a dispersion compensation glass in the reference arm. To excite the tissue, two super luminescent diodes were used with a center

wavelength of 846 nm and 932 nm. The lateral resolution was 4 μm and the axial resolution was 3.8 μm.

***In vivo* molecular imaging of choroidal neovascularization:** Before and after administration of either ultraminiature or large GNC-RGD, multimodal PAM and OCT imaging was acquired to evaluate the developed new blood vessels. All experiments were implemented as blinded and randomized analyses to eliminate bias. Twenty-four white New Zealand rabbits (~2.7–3.2 kg) were selected and utilized for all the experiments to evaluate CNV margins. Animal state was monitored through each step including temperature, mucous membrane color, heart rate, and respiratory rate were monitored and documented. Prior to each experiment, animals were anesthetized using ketamine (40 mg/kg, 100 mg/mL) and xylazine (5 mg/kg, 100 mg/mL). Rabbit eye pupils were dilated by administering 1% ophthalmic and phenylephrine hydrochloride 2.5% ophthalmic. To provide topical anesthesia, tetracaine 0.5% drops were added to the eye for comfort and reduced dehydration. A localized warming and cooling therapy system (TP-700, Stryker Corporation, Kalamazoo, MI) was used to help maintain body temperature throughout the experimentation.

Multimodal molecular images of CNV were achieved pre and post I.V. administration of GNC-RGD. After anesthetization, the animals were placed on an imaging platform to monitor the area of interest using fundus photography. The rabbit is then transferred to a different platform involving a custom-made stabilization platform with one supporting the body and another supporting the head to minimize motion artifacts. OCT was first performed, and then the ultrasound sensor was mounted in the eye chamber for PAM acquisition. The transducer was

allowed to move in three-dimensions without applying physical pressure to the rabbit eye. The region of interest for PAM imaging was selected by comparing it to the physiology visualized in fundus imaging. After control images were acquired, either ultraminiature or large GNC-RGD (0.4 mL, 5 mg/mL) were intravenously administrated into the rabbit using a 27-gauge needle. Post-injection, color photography, FA, PAM, and OCT images were acquired and followed up for 28 days. The body weight of all treated animals was measured daily post-injection. This was continued until day 28 when the rabbit models were euthanized for histological analysis.

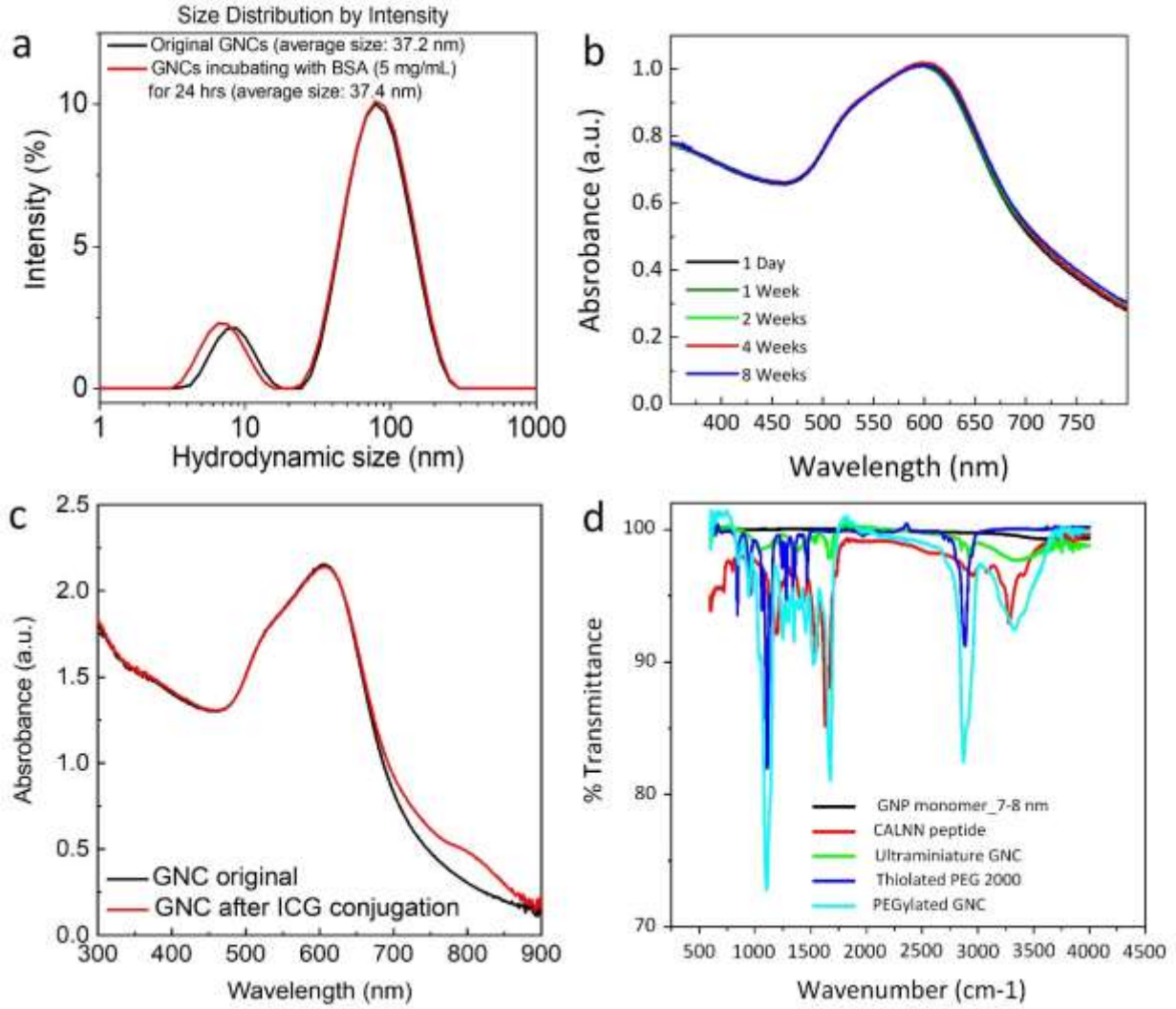

Fig. S1. Physiochemical characterization of ultraminiature GNC: (a) Comparison of hydrodynamic sizes of GNCs before and after incubating with bovine serum albumin (BSA). (b) Stability of ultraminiature GNC over time measured by UV-Vis spectrometer. There is no significant red-shift observed on the absorption spectrum of the sample up to 8 weeks. (c) Comparison of absorption spectrum of GNCs before and after ICG conjugation. (d) Fourier transformed infrared spectroscopy (FTIR) of different compounds and nanoparticles including Thiolated PEG 2000, CALNN peptide, PEGylated ultraminiature gold nanochains (GNC), ultraminiature GNC, and GNP monomer (7-8 nm in diameter).

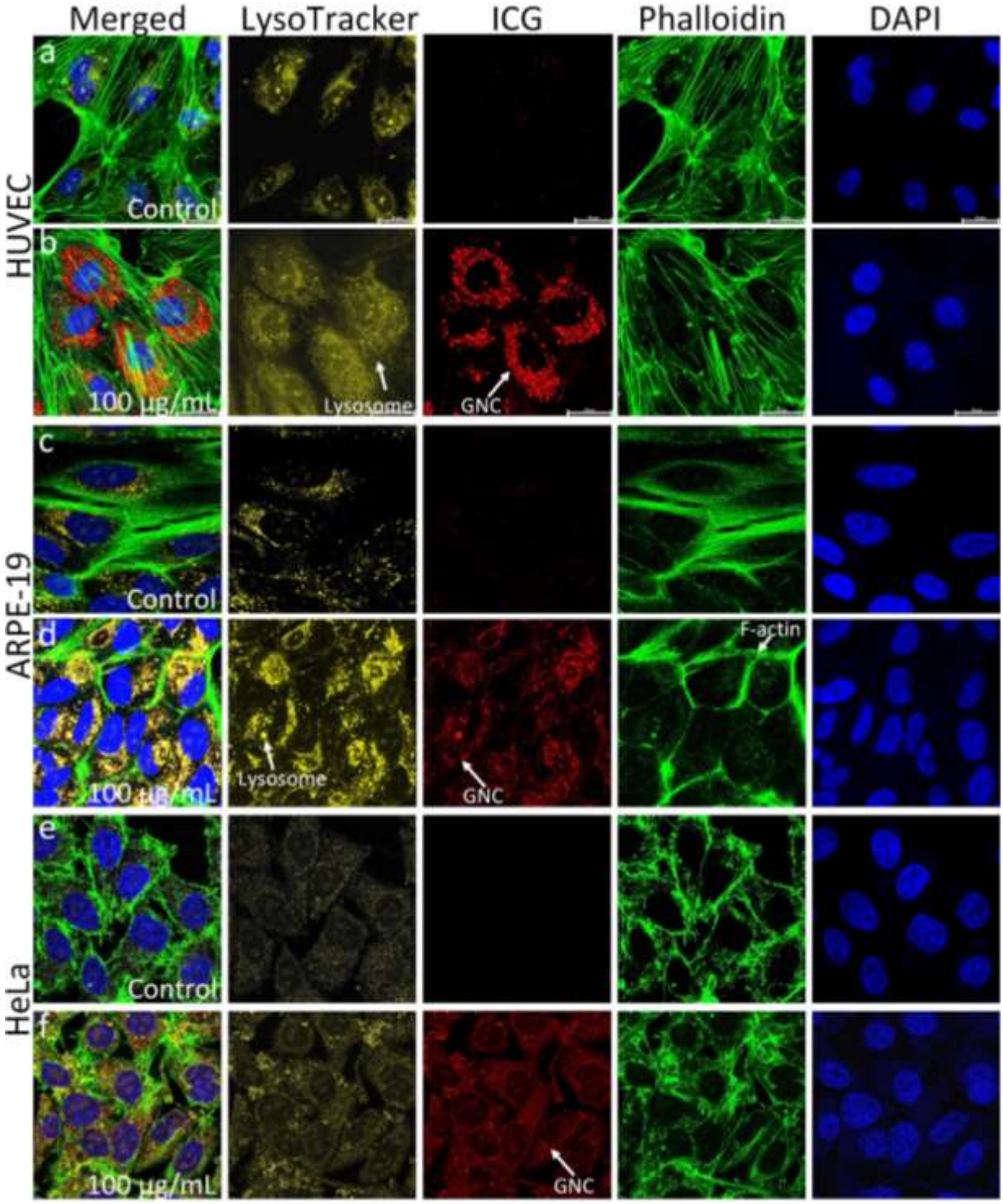

Fig. S2. Confocal laser scanning microscope analysis. (a–b) Confocal microscope image of HUVEC cells treated with 100 μg/mL ultraminiature GNC conjugated with RGD and ICG dye and with ultraminiature GNC without RGD and treated for 1 day, respectively. The cell's actin membrane, lysosome, and nucleus were monitored by phalloidin (green), LysoTracker (yellow),

and DAPI (blue). The red color indicates the detected internalized GNC inside the cells. (c–d) Confocal laser scanning pictures of ARPE-19 cells treated with ultraminiature GNC with and without targeting, respectively. (e–f) Confocal laser scanning pictures of HeLa cells treated with ultraminiature GNC with and without targeting, respectively.

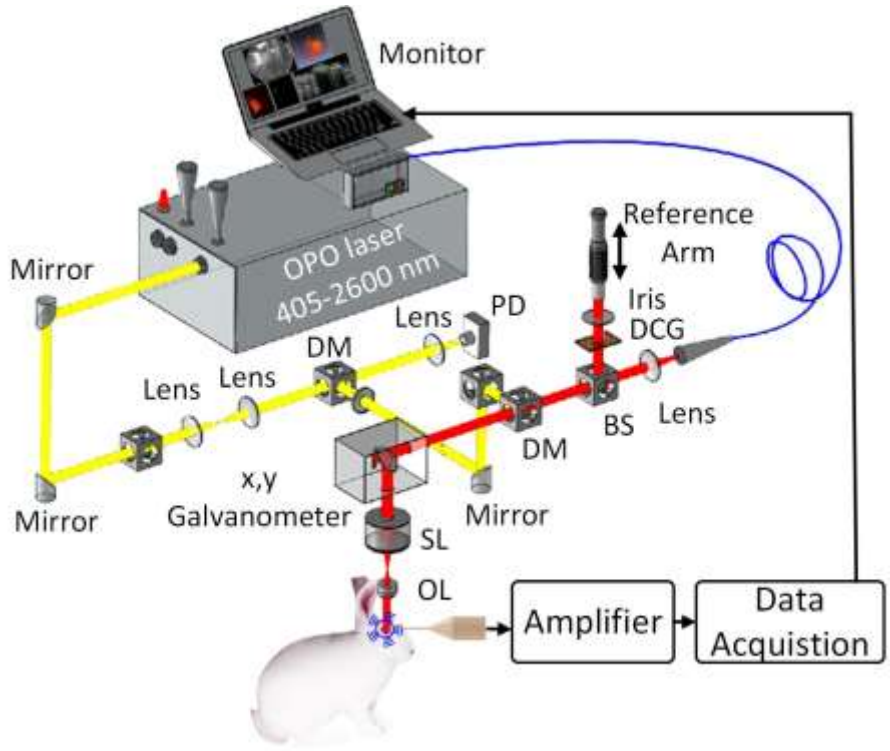

Fig. S3. Schematic of multimodal PAM and OCT imaging system.

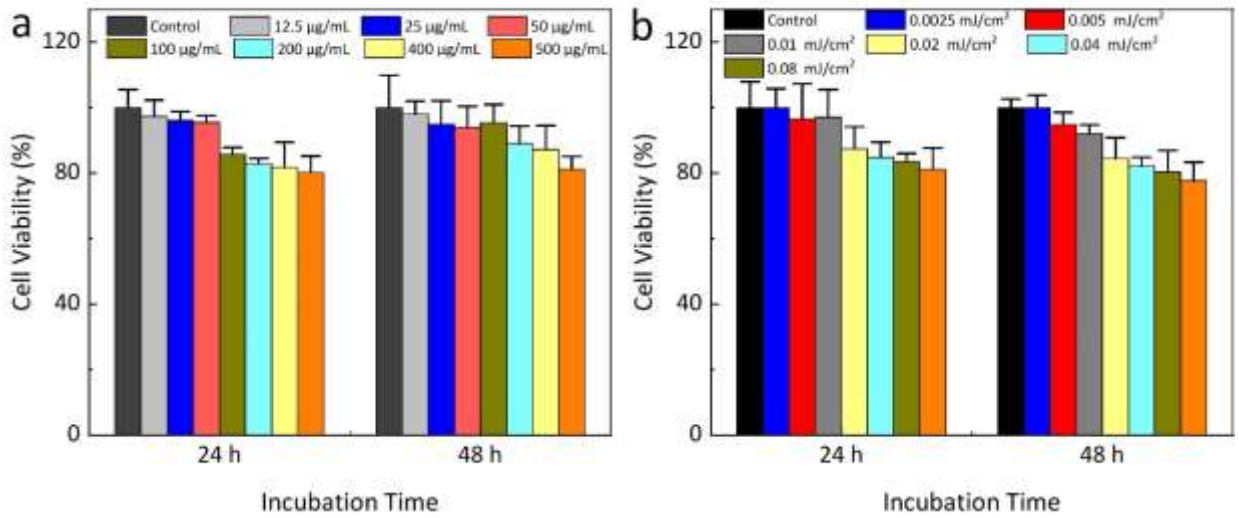

Fig. S4. Cytotoxicity results of GNC conjugated with ICG and RGD peptides using HeLa cells: (a) HeLa cells treated with GNC at different concentrations ranging from (0 (saline) to 500 µg/mL) and different incubation time of 24 hrs and 48 hrs. (b) Treated cells with GNC at final concentration of 100 µg/mL followed by laser illuminated at different laser fluences and different incubation time of 24 hrs and 48 hrs. Data presents as mean±SD (N=3, **p<0.001)

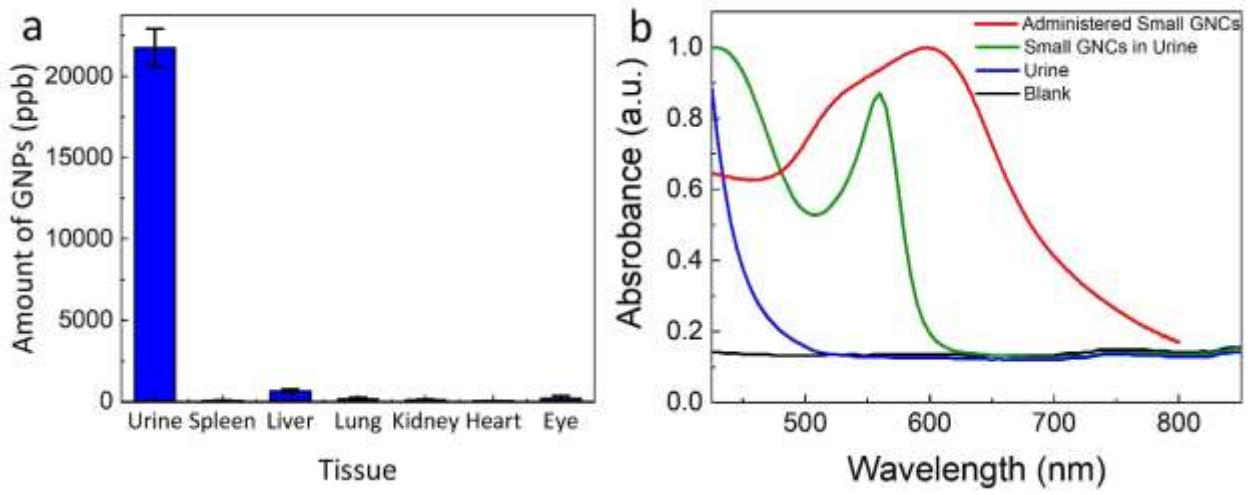

Fig. S5. Renal clearance analysis: (a) Biodistribution of ultraminiature GNC in organs harvested at 6 hrs post intravenous injection of GNC-RGD. GNC were mostly detected in urine. A small amount of GNC were also found at liver, spleen, lung, kidney, eye, and heart due to the accumulation of GNC at CNV (eye) and the presence of GNC in blood stream (heart), and in the filtration of clearance process (kidney, spleen, and liver). (b) UV-Vis absorption spectrum of urine collected after treated with and without ultraminiature GNC. The sample treated with the ultraminiature GNC show peak absorption at 550 nm which is collapsed with the absorption spectrum of monomer GNPs. This results demonstrates the clearance of the ultraminiature GNC through urine.

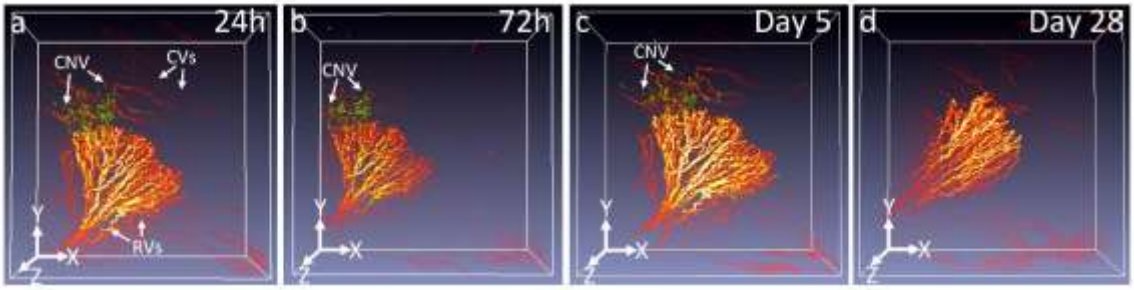

Fig. S6. Selected overlay 3D PAM data at 650 nm (green) and 578 nm (red/yellow)rendering was obtained at different time points: (a) 24 h, (b) 72 h, (c) day 5, and (d) day 28.

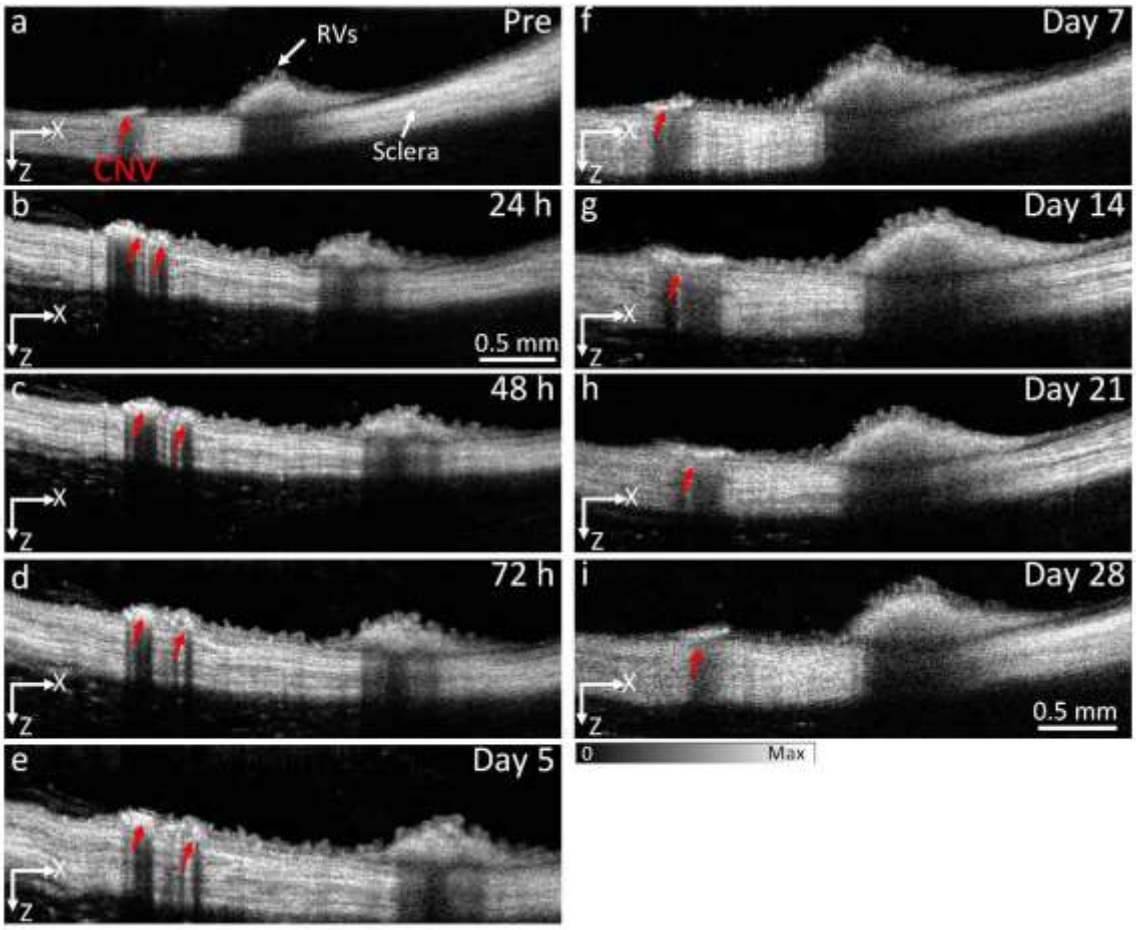

Fig. S7. Extended *in vivo* B-scan OCT was achieved pre and post administration GNC at day 1, 2, 3, 5, 7, 14, 21, and 28. Red arrows indicate the detected CNV.

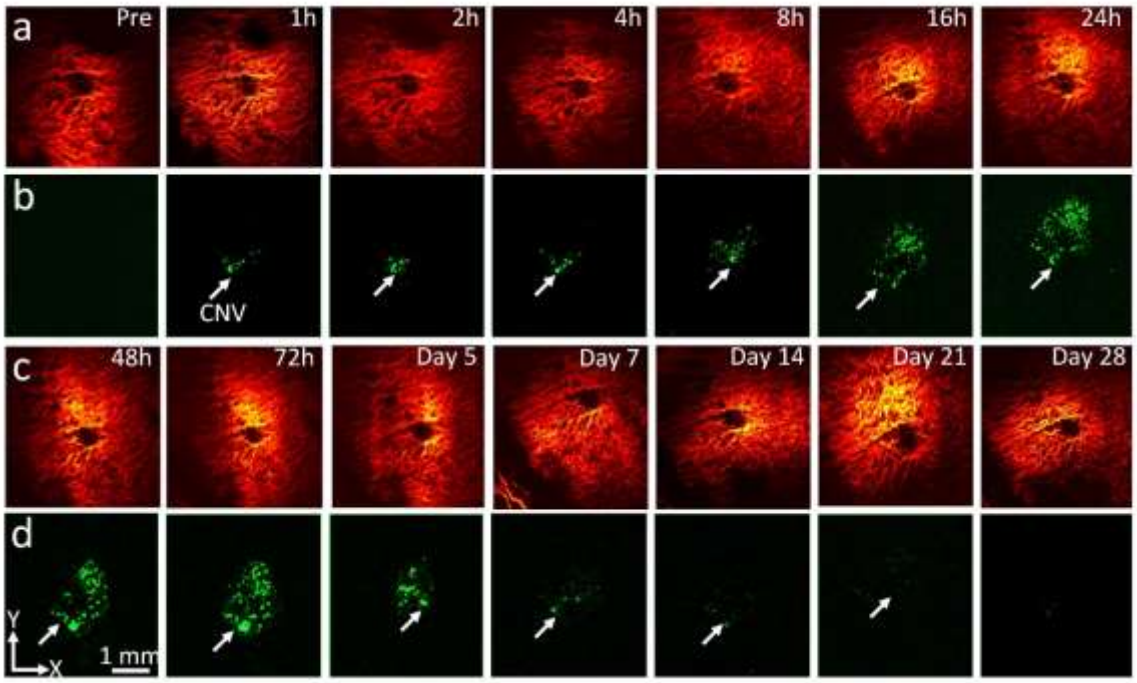

Fig. S8. Extended *in vivo* PAM images were acquired pre and at 1 h. 2 h, 4 h, 8 h, 16 h, 24 h, 48 h, 72 h, days 5, 7, 14, 21, and 28 post treatment. White arrows indicate the PA signal generated from the accumulation of GNC at CNV.

Table. S1. Liver and kidney function tests on mice at low concentrations (2.5-20 mg/kg)

Test	Normal Range	Unit	Control	2.5 mg/kg	5.0 mg/kg	10 mg/kg	20 mg/kg
Liver Function Tests (LFT)							
Total Protein (TPRO)	4.63-7.2	g/dL	4.83±0.55	4.93±0.21	4.70±0.36	5.20±0.26	5.40±0.36
Alanine aminotransferase (ALT)	24.30-115.25	U/L	46.67±10.69	27.67±7.23	30.33±4.93	36.00±9.54	31.33±1.53
Total Bilirubin (TBIL)	0.12-0.58	mg/dL	0.18±0.01	0.23±0.02	0.14±0.07	0.17±0.02	0.13±0.06
Alkaline phosphatase (ALP)	65.50-364.20	U/L	120.67±17.79	99.33±10.79	80.33±11.59	167.67±114.33	114.33±65.45
Albumin (ALB)	2.72-4.2	g/dL	3.13±0.35	2.77±0.06	2.63±0.21	2.83±0.15	2.90±0.10
Kidney Function Tests (KFT)							
Blood urea nitrogen (BUN)	5.15-30.7	mg/dL	28.00±3.61	20.00±2.00	24.33±3.21	21.67±2.89	29.00±1.00
Creatinine (CREA)	0.09-0.4	mg/dL	0.28±0.04	0.18±0.03	0.28±0.01	0.29±0.07	0.25±0.05

Table. S2. Liver and kidney function tests on rabbits at low concentrations

Test	Normal Range	Unit	Control	Ultraminiature GNC	Large GNC	Large GNS
Liver Function Tests (LFT)						
Total Protein (TPRO)	5.0-7.5	g/dL	6.6±0.3	5.8 ± 0.5	7.1±2.3	6.3±2.8
Alanine aminotransferase (ALT)	25-65	U/L	35±3.2	39.7 ± 4.2	42±7.8	55±4.7
Total Bilirubin (TBIL)	0.2-0.5	mg/dL	0.4±0.05	0.3 ± 0.1	0.2±0.07	0.32±0.3
Alkaline phosphatase (ALP)	10.0-86.0	U/L	80±8.3	76.0 ± 10.0	83±9.1	75±5.8
Albumin (ALB)	2.7-5.0	g/dL	4.4±0.1	4.0 ± 0.3	3.8±0.2	3.8±1.5
Kidney Function Tests (KFT)						
Blood urea nitrogen (BUN)	5.0-25.0	mg/dL	23±3.3	19 ± 3.5	18±2.3	17±2.6
Creatinine (CREA)	0.5-2.6	mg/dL	1.35±0.4	0.8 ± 0.2	2.2±0.8	1.72±1.11

Table. S3. Liver and kidney function tests on mice at high concentrations (2200-8800 mg/kg)

Test	Normal Range	Unit	Control	Ultraminiature GNC		Large GNC	
				2200 mg/kg	8800 mg/kg	2200 mg/kg	8800 mg/kg
Liver Function Tests (LFT)							
Total Protein (TPRO)	4.63-7.2	g/dL	4.83±0.55	3.56±3.02	5.25±0.21	5.77±0.57	5.15±0.35
Alanine aminotransferase (ALT)	24.30-115.25	U/L	46.67±10.69	54.00±26.06	118.00±109.12	22.67±1.15	37.67±0.58
Total Bilirubin (TBIL)	0.12-0.58	mg/dL	0.18±0.01	0.14±0.03	0.22±0.05	0.14±0.02	0.15±0.04
Alkaline phosphatase (ALP)	65.50-364.20	U/L	120.67±17.79	123.33±35.56	107.33±5.69	133.67±14.43	96.67±23.12
Albumin (ALB)	2.72-4.2	g/dL	3.13±0.35	3.47±0.59	3.87±0.61	4.30±0.20	4.70±0.10
Kidney Function Tests (KFT)							
Blood urea nitrogen (BUN)	5.15-30.7	mg/dL	28.00±3.61	29.67±2.52	30.33±8.14	30.67±5.51	46.00±16.46
Creatinine (CREA)	0.09-0.4	mg/dL	0.28±0.04	0.21±0.04	0.25±0.12	0.27±0.03	0.23±0.03

SUPPLEMENTARY MOVIE CAPTIONS

Movie S1. Animated representation of 3D volumetric rendered PAM images is shown in Figure 5h.

Movie S2. Fly-through of the depth-encoded image is represented in Figure 5k.

Movie S3. Animated 3D volumetric PAM rendering obtained at 48 h post-administration of ultraminiature GNC is shown in Figure 9h.

Supplementary References

1. B. Liu, Z. Hu, M. Murakami, Y. Che, Google patents. (2012).
2. B. Liu, Z. Hu, Y. Che, Y. Chen, X. Pan, Nanoparticle generation in ultrafast pulsed laser ablation of nickel. Applied Physics Letters 90, 044103 (2007).
3. J.-P. Sylvestre, S. Poulin, A. V. Kabashin, E. Sacher, M. Meunier, J. H. Luong, Surface chemistry of gold nanoparticles produced by laser ablation in aqueous media. The Journal of Physical Chemistry B 108, 16864-16869 (2004).
4. R. Lévy, N. T. Thanh, R. C. Doty, I. Hussain, R. J. Nichols, D. J. Schiffrin, M. Brust, D. G. Fernig, Rational and combinatorial design of peptide capping ligands for gold nanoparticles. J. Am. Chem. Soc. 126, 10076-10084 (2004).
5. A. E. Nel, L. Mädler, D. Velegol, T. Xia, E. Hoek, P. Somasundaran, F. Klaessig, V. Castranova, M. Thompson, Understanding biophysicochemical interactions at the nano–bio interface. Nature materials 8, 543-557 (2009).

6. M. Oncel, G. A. Peyman, B. Khoobehi, Tissue plasminogen activator in the treatment of experimental retinal vein occlusion. Retina 9, 1-7 (1989).
7. V. P. Nguyen, W. Qian, Y. Li, B. Liu, M. Aaberg, J. Henry, W. Zhang, X. Wang, Y. M. Paulus, Chain-like gold nanoparticle clusters for multimodal photoacoustic microscopy and optical coherence tomography enhanced molecular imaging. Nature Communications, 12(1), 1-14 (2021).
8. V.P. Nguyen, W. Fan, T. Zhu, W. Qian, Y. Li, B. Liu, W. Zhang, J. Henry, S. Yuan, X. Wang, Y.M. Paulus, Long-Term, Noninvasive In Vivo Tracking of Progenitor Cells Using Multimodality Photoacoustic, Optical Coherence Tomography, and Fluorescence Imaging. ACS nano. Aug 11;15(8):13289-306 (2021).